Journal of Alloys and Compounds 694 (2017) 253–260

Contents lists available at ScienceDirect

Journal of Alloys and Compounds

journal homepage: http://www.elsevier.com/locate/jalcom

Effects of chemical potential on the thermoelectric performance of alkaline-earth based skutterudites (AFe_4Sb_{12}, A=Ca, Sr and Ba)

Banaras Khan [a, b, *], M. Yazdani-Kachoei [c, **], H.A. Rahnamaye Aliabad [d], Imad Khan [a, b], S. Jalali-Asadabadi [c], Iftikhar Ahmad [a, e]

[a] Center for Computational Materials Science, University of Malakand, Chakdara, Pakistan
[b] Department of Physics, University of Malakand, Chakdara, Pakistan
[c] Department of Physics, Faculty of Sciences, University of Isfahan (UI), Hezar Gerib Avenue, 81746-73441 Isfahan, Iran
[d] Department of Physics, Hakim Sabzevari University, Sabzevar, Iran
[e] Abbottabad University of Science and Technology, Abbottabad, Pakistan

ARTICLE INFO

Article history:
Received 26 June 2016
Received in revised form
22 September 2016
Accepted 28 September 2016
Available online 3 October 2016

Keywords:
Skutterudites
Electronic structure
Thermoelectric materials
Boltzmann's theory

ABSTRACT

In this paper we explore the electronic nature and thermoelectric properties of filled skutterudites AFe_4Sb_{12} (A=Ca, Sr and Ba) by DFT and post-DFT techniques. The calculated results show that the filling of Ca, Sr, and Ba at the empty crystal sites enhances the thermoelectric performance of the host material. This increase is a consequence of the coupling between the guest and the host atoms, which affects the electronic density at different symmetry points that increases the density of states of the valence bands. The valence band edge is almost independent of the guest atoms, i.e., the s-bands of Ca, Sr and Ba have negligibly small contribution to the valence band edge. In these compounds, the maximum value of thermoelectric PF/τ of 42.43×10^{14} $\mu W/cmK^2s$ and 33.57×10^{14} $\mu W/cmK^2s$ for the n-type of $SrFe_4Sb_{12}$ in the spin-up and down states respectively. The striking feature of these compounds is their effectiveness at the low chemical potential values for the best thermoelectric performance.

1. Introduction

In thermoelectric power generators, heat energy is used to push electrons and holes in opposite directions in thermoelectric (TE) materials. These generators are highly reliable for their static nature with no moving parts. The progress in the search for high performance TE materials may ultimately lead to efficient TE material that can save most of the heat losses by transferring waste heat to electricity [1]. In the recent years, focus on the promising thermoelectric materials is enhanced to overcome the energy crises by converting waste heat into electricity [2–4].

The efficiency of a TE material can be quantified by the relation $ZT = S^2\sigma T/\kappa$, where S is the Seebeck coefficient, σ is the electrical conductivity and κ is the thermal conductivity of a material at a given temperature T [5]. The search for the efficient TE materials has led to numerous advances which have resulted in enhanced ZT values for different types of compounds including superlattices, nanostructured materials, nanocomposites, and bulk materials [6–19]. It is evident that in all these types of materials, the TE parameters such as S, σ, and κ are strongly interdependent on each other. For example, compounds having high Seebeck values usually have low values of electrical conductivity and high values of thermal conductivity. These intrinsic properties restrict the spontaneous optimization of electrical and thermal transport properties of a compound, as well as its ZT value [20].

Binary skutterudite compounds MX_3 (M=Co, Rh, or Ir; X=P, As, or Sb) have cage-like crystallographic nature due to their corner sharing MX_6 octahedral [21–23]. Among the binary skutterudites $CoSb_3$ is an exemplary skutterudite system as it has excellent electronic properties with high Seebeck coefficient [23]. However, the main issue with $CoSb_3$ is that its thermal conductivity is too large which restricts the optimization for achieving a high thermoelectric efficiency [21–23]. Also the ability to lower the thermal conductivity in $CoSb_3$ by using filler atoms is limited [24], since the filling factor is rather small and focus on filled skutterudites has been directed towards other skutterudites, such as Fe containing

* Corresponding author. Department of Physics, University of Malakand, Chakdara, Pakistan.
** Corresponding author.
E-mail addresses: banarasphysicist@gmail.com (B. Khan), yk.majid@gmail.com (M. Yazdani-Kachoei).

http://dx.doi.org/10.1016/j.jallcom.2016.09.308
0925-8388/

$R_yFe_xCo_{1-x}Sb_{12}$. The filling factor is larger for such systems and for $R_yFe_4Sb_{12}$ the filling factor reaches unity [25–29].

The empirical formula of the filled skutterudites is RM_4Sb_{12}, where R can be alkali, alkaline-earth, lanthanide, or actinide metals, and M is Fe, Ru, Os, Co, Rh, or Ir. The studies on the thermoelectric properties of the filled skutterudites were initially started in the last decades of the twentieth century [14,22,30–34]. In this era the main focus was on the p-type partially filled Fe based skutterudites compounds and the dimensionless figure of merits for these materials were reported above unity [31,32,35,36]. Research work on the n-type filled skutterudites was rather slow, until partially filled skutterudites with high filling fraction of the fillers were synthesized and reported with good thermoelectric performance at high temperatures [37–39]. Since then, the thermoelectric figure of merit of the n-type skutterudites has also gained interest in various n-type single element filled skutterudites with high ZT values [40,41]. The filling of two or more types of fillers into the voids in skutterudite has shown further reduction in the lattice thermal conductivity and hence improvement in the ZT to 1.4 in double-filled and 1.7 in multiple-filled n-type skutterudites [15,42,43]. Although there are a series of recent studies with high ZTs in n-type partially filled skutterudites but only a few studies show high temperature thermoelectric properties in the p-type skutterudites. Furthermore, the ZT values of the p-type filled skutterudites are confirmed in experiments and they are around 1.0, i.e., much lower than n-type materials [44–46]. The stagnation of low ZT value in the p-type skutterudites restricts the further development of thermoelectric devices, since both excellent n- and p-type materials are required for high efficiency thermoelectric technology. Hence, search for p-type skutterudites with comparable ZT values to n-type materials is the need of the time for industrial applications.

Fully filled skutterudites RFe_4Sb_{12} are important p-type skutterudites, where the first RFe_4Sb_{12} compound was initially reported in 1980 [47]. After that, various RFe_4Sb_{12} ternary compounds with different filler elements were synthesized and many interesting physical properties were reported for them [22,30,32–34,48–58]. However, the thermoelectric properties have been studied for a few RFe_4Sb_{12} compounds experimentally [22,32,34,40,52]. Furthermore, high temperature thermoelectric properties, which are crucial for the thermoelectric power generator, have been rarely reported in RFe_4Sb_{12} [32,34,40]. Due to the lack of a broad systematic study, a detailed theoretical understanding of the electrical and thermal transport properties in alkaline-earth based AFe_4Sb_{12} systems is still not available in the literature, which hinders the further optimization to achieve high ZT in these compounds. Therefore, it is essential to gain a comprehensive understanding of the electrical and thermal transport properties of alkaline-earth elements filled AFe_4Sb_{12} skutterudites.

In this paper, a series of AFe_4Sb_{12} samples with various fillers (A=Ca, Sr and Ba) are modeled and their thermoelectric properties are calculated for different chemical potential values at room temperature. Hence, we carry out a systematic evaluation and discuss the thermoelectric properties of these compounds related to their chemical potentials.

2. Theory and calculations

The electronic structures of AFe_4Sb_{12} (A=Ca, Sr and Ba) compounds are calculated using the full-potential linearized augmented plane waves (FPLAPW) method. The basis functions, i.e., the LAPWs, are composed of linear combinations of an APW and a local orbital (LO). For the exchange-correlation potential, the PBEsol08 GGA is used in the self-consistent field (SCF) calculations [59]. Following this method, there is no restriction on the shape approximation wether on potential or on the electronic density. The space of the cell is divided into interstitial (IR) and muffin-tin (MT) regions, however, the MTs have localization at the atomic positions. The basis set in the interstitial regions is made of plane waves, whereas the MT spheres bases set is given by the solutions of the radial Schrödinger equation and related energy derivatives which are multiplied by lattice harmonics. All these assumptions and related parameterization are fixed in the WIEN2k code [60]. In our case, for the electronic structure calculations, 1000 k-points are used in the first Brillouin zone, and the cutoff parameter is taken $R_{MT}K_{max} = 7$, where K_{max} is the maximal value of the reciprocal lattice vector of the plane wave expansion, and R_{MT} is the smallest atomic sphere radius in the unit cell. These calculations have been done in the presence of spin polarization and absence of spin-orbit coupling.

Using the calculated band structure, the thermoelectric transport tensors can be evaluated through the Boltzmann's transport theory [61] Thermoelectric calculations require a denser k-mesh for the convergence. Thus, we used a high dense k-mesh of 150000 k-points for the transport properties convergence. This k-mesh is more than 150 times denser than that used for the electronic structure calculations as mentioned by Madsen and Singh [62]. Boltzmann's transport theory calculates the thermoelectric transport parameters as implemented in the BoltzTraP code [62,63]. The BoltzTraP code is a computational tool based on the smooth Fourier interpolations of the band energies. The code uses the interpolated band structure by WIEN2k to calculate the derivatives necessary to evaluate the transport properties. Using this approach, Seebeck coefficient, electrical and thermal conductivity relative to relaxation time τ are calculated without any fitting parameter. Furthermore, the BoltzTraP code is based on the relaxation time approximation. According to Ref. [64], this approximation is valid for high doping level $> 10^{18}/cm^3$. The relaxation time (τ) is considered constant during the calculation of this code; however, its magnitude is not fixed and has not a default value. The Seebeck coefficient does not depend on the value of the relaxation time. The electrical and thermal conductivity that depend on the relaxation time are presented as σ/τ and κ/τ, as shown in Figs. 5 and 6. The value of relaxation time can be determined by comparing the theoretical results with the available experimental data as done in Ref. [65].

The Seebeck coefficient, S, electrical conductivity, σ, and, electronic contribution to the thermal conductivity, κ_e, tensors can be expressed as follows

$$S = ek_B\sigma^{-1}\sum k\left(-\frac{df_0}{d\varepsilon}\right)\upsilon_k^2\tau_k\frac{k_B-\mu}{k_BT}, \quad (1)$$

$$\sigma = e^2\sum k\left(-\frac{df_0}{d\varepsilon}\right)\upsilon_k^2\tau_k, \quad (2)$$

$$k_e = ek_B\sigma^{-1}\sum k\left(-\frac{df_0}{d\varepsilon}\right)\upsilon_k^2\tau_k\left(\frac{k_B-\mu}{k_BT}\right)^2 - T\sigma S^2, \quad (3)$$

where e is the charge of carrier, k_B is the Boltzmann's constant, f_0 is the Fermi distribution function,υ_k is the group velocity, τ_k is the relaxation time, ε is the energy, andμ denotes the chemical potential. From the solutions of Eqs. (1)–(3), we can estimate the transport coefficients and thereby obtain the PF of a compound. The doping levels can be evaluated by changing the Fermi level (E_F) to obtain the n- or p-doped materials. The key parameters used in BoltzTraP for the calculations are Fermi level, delta, ecut, number of valence electrons, energy span around the Fermi level, T_{max} and temperature grid. The delta 0.0001, ecut 0.15, number of valence

electrons 326, energy span around the Fermi level 0.5, T_{max} 500 K, temperature grid 1 K values have been used for each of the compounds $CaFe_4Sb_{12}$, $SrFe_4Sb_{12}$ and $BaFe_4Sb_{12}$. However, the Fermi energies 0.55978 Ry, 0.56865 Ry and 0.58281 Ry as obtained from the band structure calculations are used for the thermoelectric calculations of $CaFe_4Sb_{12}$, $SrFe_4Sb_{12}$ and $BaFe_4Sb_{12}$, respectively.

3. Results and discussions

3.1. Electronic structure

It has been observed that efficient thermoelectric compounds are usually narrow band gap semiconductors with dense electronic states around the Fermi levels. Thus, we performed the electronic structure calculations of $CaFe_4Sb_{12}$, $SrFe_4Sb_{12}$ and $BaFe_4Sb_{12}$ compounds, focusing on their band structure around the Fermi levels, as our first criterion. The crystal structure for each compounds presented in Fig. 1, is optimized. The crystal structure shows the cage-like structure of the skutterudite unit cell with the filling of alkaline-earth element. In our calculations, the alkaline-earths fully occupy the 2a sites, Fe occupies the 8c and Sb occupies the 24*g* of the crystallographic positions. However, it is experimentally established that alkaline-earth element doesn't fully occupy the 2*a*-voids and occupancy factor is usually less than 1. A detailed description of the electronic structures of the alkaline-earth based filled skutterudite systems for spin-up and spin-down states can be seen in Fig. 2. We used PBE-sol08 GGA for the electronic structure calculations in the presence of spin polarization which underestimate the band gap, however, it is realistic to use this potential because of the metallic nature of the compounds as confirmed from experimental results [64]. At first glance from left panel of Fig. 2 it appears that both spin up and spin down band structures of the compounds under question behave as semiconductors at Δ,*H*,*N*,$\sum$,Λ and *P* symmetry points, see Fig. 2 (a) − (f). Namely, it appears that there is only a single multiple degenerate band that crosses the Fermi Level at Γ symmetry point for both of the up and down channels. Thus, for sure the band structures are magnified nearby the Fermi level in the right panel of Fig. 2 for both spin up and down channels; see Fig. 2 (m1) and (m2). As can be clearly seen from these magnified band structures, however, these compounds are all behave as metallic systems. The band crossing is justified from the available literature which indicates metallic nature of these compounds as reported experimentally [58]. Cheng et al. [65] performed electronic structure calculations by LSDA and obtained results, which show that $BaFe_4Sb_{12}$ was half metal whereas calculations performed by Zhou [66] and Schnelle [67] show the similar electronic structure as investigated in our calculations. In these compounds since the band gap is non-existent therefore minority carriers are likely to play a major role close to the Fermi level. Total and partial up and down densities of states are shown in Fig. 3 for $CaFe_4Sb_{12}$, $SrFe_4Sb_{12}$ and $BaFe_4Sb_{12}$ around the Fermi level. In these figures the vertical dotted line denotes the Fermi level. The band crossing can be clearly observed by the down partial and total DOSs, as shown in Fig. 3 (b) and (d), respectively. However, it hard to see the band crossing by looking at the up partial and total DOSs, as shown in Fig. 3 (a) and (c), respectively. Therefore, the up and down p-DOSs are magnified by zooming the DOSs very close to the Fermi level, as shown in Fig. 3 (m1) and (m2). The zoomed figures clearly show that both of the up and down DOSs cross the Fermi level. This once more in consistent with our band structure results and in complete accord with Ref. [67] elucidates that these compounds would behave as nearly ferromagnetic metals, which is in contrast to the half-metallic behavior reported in Ref. [65]. It is clear from the Fig. 3 that electronic states around the Fermi level are extremely dense which play a vital role for the good thermoelectric nature of these materials. The partial DOS for each element is a sum of a partial DOS over all muffin-tin spheres of the same compound. Since the electronic structure near the Fermi energy is significant for thermoelectric properties, we discuss the electronic structure near the band edges. The overall shapes of electronic structures of $CaFe_4Sb_{12}$, $SrFe_4Sb_{12}$ and $BaFe_4Sb_{12}$ are similar except for Ca, Sr and Ba contributions in $CaFe_4Sb_{12}$, $SrFe_4Sb_{12}$ and $BaFe_4Sb_{12}$. The top of the valence band is composed of s-Ca, p-Sb and 3d-Fe states with parabolic energy dispersion, especially small contribution of the s-Ca, p-Sb states on the Fe atom. The contribution of 3d-Fe state to the valence band edge is large due to the fact that its density of states is located very close to the Fermi level, so it has major impact on the thermoelectric performance of the materials. Spin-orbit coupling and crystalline electric field effects are not included in the calculations, however, it is expected that inclusion of spin-orbit coupling and crystalline electric field splits the states and reductions in the peaks of density of states occur around the Fermi level, which result in the decrease in the thermoelectric parameters of these materials.

3.2. Seebeck coefficient

Seebeck coefficient is the most fundamental parameter to understand the response of a material to the applied temperature gradient. Seebeck coefficient with reference to chemical potential is negative for n-doped and is positive for p-doped systems. Chemical potential defines the doping level or carrier concentration in a material, which is very important for enhancing the thermoelectric nature of a material for practical realization.

"However, we should keep in mind that the magnitude of the charge carrier concentration corresponding to the chemical potential depends on the actual band structure, which are not claimed

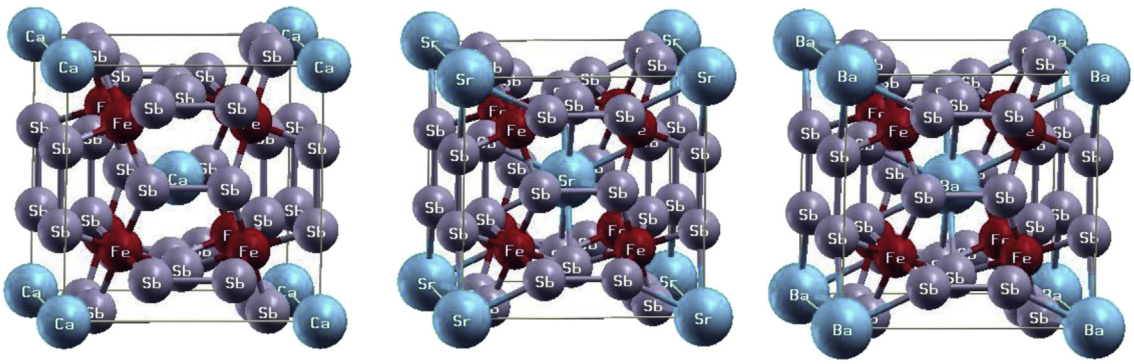

Fig. 1. Crystal structure of AFe_4Sb_{12}(A=Ca, Sr and Ba) showing cage-like structure and inserted alkaline-earth atoms.

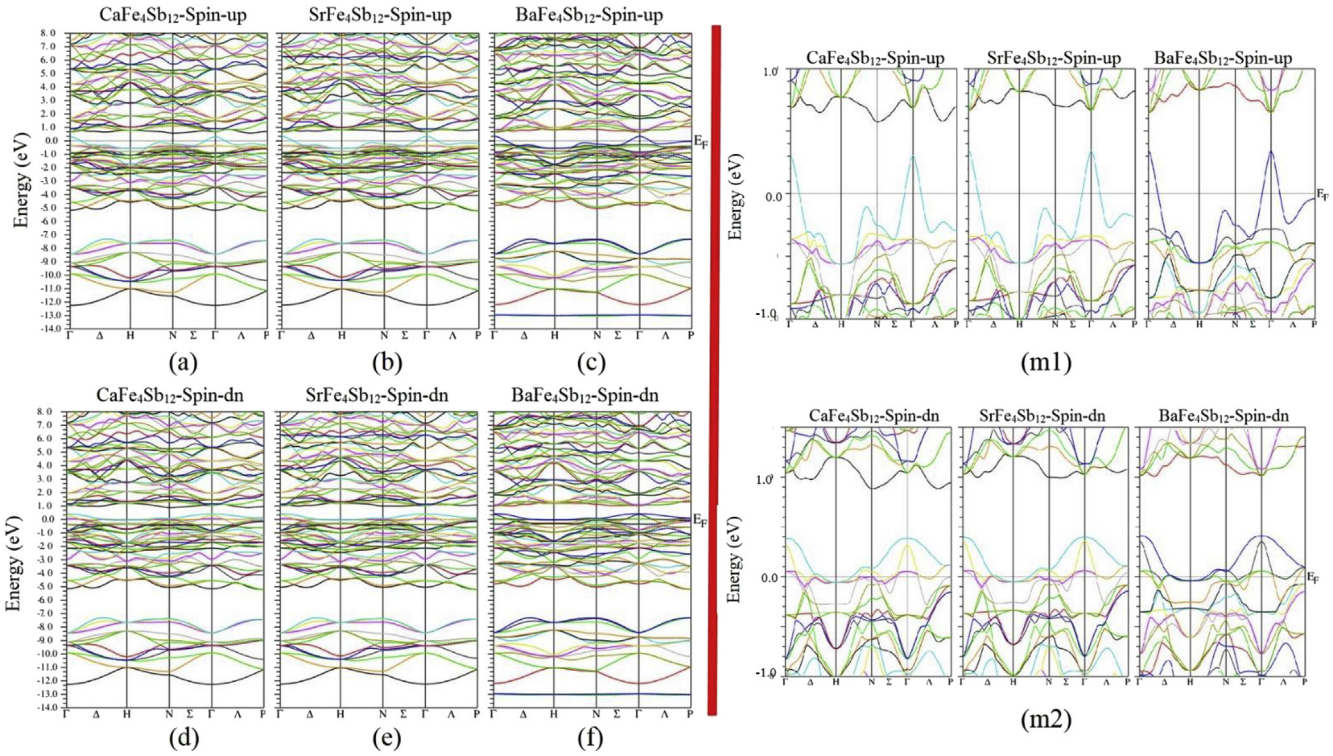

Fig. 2. Left panel shows spin up band structures for the filled skutterudites (a) $CaFe_4Sb_{12}$, (b) $SrFe_4Sb_{12}$, and (c) $BaFe_4Sb_{12}$. Spin down band structures for the filled skutterudites (c) $CaFe_4Sb_{12}$, (d) $SrFe_4Sb_{12}$, and (e) $BaFe_4Sb_{12}$. Fermi level is set to zero. Right panel shows the magnified band structures of $CaFe_4Sb_{12}$, $SrFe_4Sb_{12}$ and $BaFe_4Sb_{12}$ for (m1) spin up and (m2) spin down states. Fermi levels are shown by horizontal solid lines and set to zero in these figures.

to be exactly predicted by the single particle DFT calculations."

The Seebeck coefficients S of spin up and down of three considered compounds are plotted against the chemical potential at room temperature as shown in Fig. 4(a) and (b). Comparing Fig. 4(a) and (b) reveals that for all of the compounds under consideration and in the both p-type and n-type regions the maximum value of Seebeck coefficient of spin down is more than 2 times larger in magnitude compared to that of the spin up. This result can be explained by the very higher value of spin down DOSs of all compounds compared to the spin up near the Fermi level. In other words, the higher value of Seebeck coefficient for carriers with spin down than those with spin up can be considered as a result of the higher value of spin down DOSs than spin up DOSs near the Fermi level. The Seebeck coefficients value obtained in p-type region for $BaFe_4Sb_{12}$ is higher than that of $CaFe_4Sb_{12}$ and $SrFe_4Sb_{12}$ for both spin up and down, which indicate that the holes contribution in p-type region is more for $BaFe_4Sb_{12}$.

In p-type region the highest value of Seebeck coefficient of spin up for $BaFe_4Sb_{12}$ is 431 μV/K, then the Seebeck coefficient of $SrFe_4Sb_{12}$ is 368 μV/K, and finally maximum Seebeck coefficient is for $CaFe_4Sb_{12}$ with the peak value of 224 μV/K. For the spin down calculations, the highest values of Seebeck coefficient in the p-type region for $BaFe_4Sb_{12}$, $SrFe_4Sb_{12}$, and $CaFe_4Sb_{12}$ are 907 μV/K, 868 μV/K, and 691 μV/K, respectively.

Similarly in the n-type region, the same characteristics of the Seebeck coefficient values are obtained and compounds favor low doping, however, high Seebeck coefficient values are obtained in n-type region than p-type which indicates the prominence of n-type on p-type doping in these materials. The maximal values of the calculated Seebeck coefficient in the n-type region for spin up (spin down) are −491 (−812) μV/K, −703 (−1026) μV/K, −681 (−1039) μV/K for $CaFe_4Sb_{12}$, $SrFe_4Sb_{12}$ and $BaFe_4Sb_{12}$, respectively. This indicates that n-doping of $SrFe_4Sb_{12}$ ($BaFe_4Sb_{12}$) is more suitable for enhancing the Seebeck coefficient of spin up (spin down) states. The high value of Seebeck coefficient in our calculations can be related to the calculated parabolic band structures due to Fe-3d states near the E_F with high effective mass which would be greater in $BaFe_4Sb_{12}$.

3.3. Electrical conductivity

Electrical conductivity in materials arose both due to holes and electrons. In metals, the dominant part is due to electrons whereas in semiconductor both holes and electrons contribute to the electrical conductivity. The electronic structures of materials underpin transport properties which are important to its use as the thermoelectric materials and large free carriers result in good conductors. Here, we have calculated the electronic structure of AFe_4Sb_{12} (A=Ca, Sr and Ba) in the ordered olivine electrical conductivity of the materials. The electrical conductivities per relaxation time (σ/τ) against the chemical potential for materials $CaFe_4Sb_{12}$, $SrFe_4Sb_{12}$ and $BaFe_4Sb_{12}$ are shown in Fig. 5 for both spin up and down, where chemical potential represents doping or the charge carrier concentration. It is clear from the figure that σ/τ is high in highly doped region for p-type and also for n-type, however, σ/τ is higher in n-type region compared to p-type due to the large carrier concentration in the valence band compared to the conduction band. The σ/τ in these materials for the p-type $BaFe_4Sb_{12}$ at 300 K decreases as holes concentration decreases. In the p-type region the maximum for spin up (spin down), σ/τ values for $CaFe_4Sb_{12}$ is 1.60×10^{20} 1/Ωms (1.88×10^{20} 1/Ωms) followed by $SrFe_4Sb_{12}$ 1.56×10^{20} 1/Ωms (1.70×10^{20} 1/Ωms) and $BaFe_4Sb_{12}$ 1.56×10^{20} 1/Ωms (1.60×10^{20} 1/Ωms), respectively. For n-type at 300 K, as chemical potential increases, there is abrupt increase for

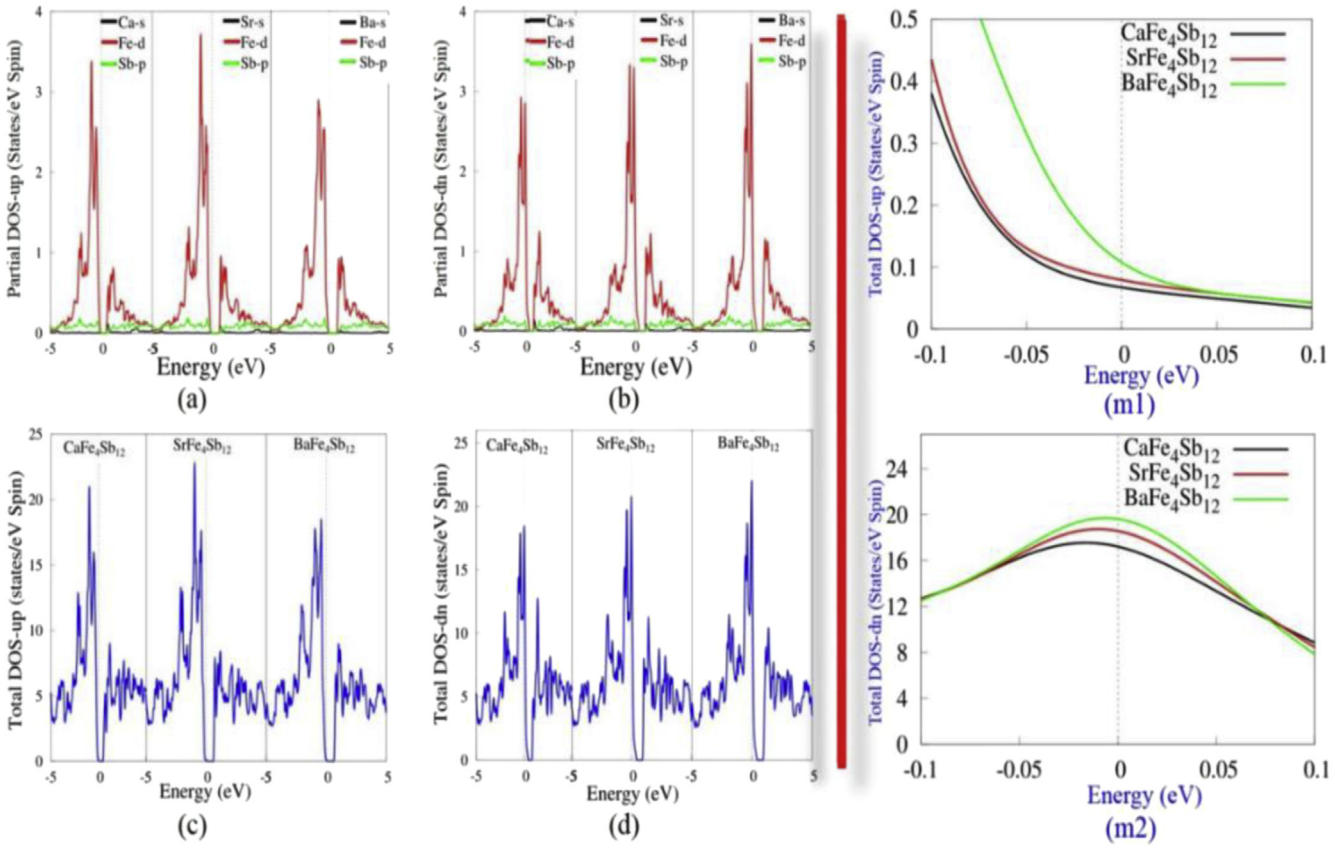

Fig. 3. Left panel shows partial densities of States of $CaFe_4Sb_{12}$, $SrFe_4Sb_{12}$ and $BaFe_4Sb_{12}$ for (a) spin up and (b) spin down and total densities of States of $CaFe_4Sb_{12}$, $SrFe_4Sb_{12}$ and $BaFe_4Sb_{12}$ for (c) spin up states and (d) spin down states. Right panel shows the magnified total densities of States of $CaFe_4Sb_{12}$, $SrFe_4Sb_{12}$ and $BaFe_4Sb_{12}$ for (m1) spin up states and (m2) spin down states. Fermi levels are shown by dotted lines and set to zero in these figures.

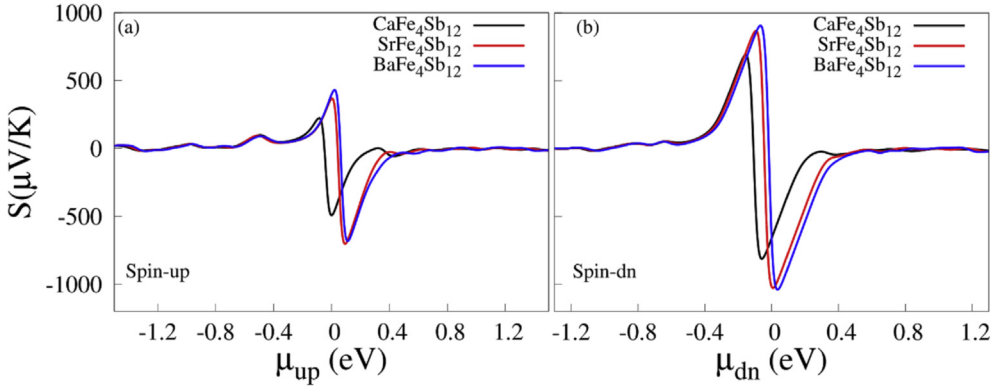

Fig. 4. Seebeck coefficients of $CaFe_4Sb_{12}$, $SrFe_4Sb_{12}$ and $BaFe_4Sb_{12}$ versus chemical potential at 300 K for (a) spin up states and (b) spin down states.

all compounds with prominent increase for $BaFe_4Sb_{12}$ than $CaFe_4Sb_{12}$ and $SrFe_4Sb_{12}$. The maximum obtained value of σ/τ for $BaFe_4Sb_{12}$ is 2.94×10^{20} 1/Ωms (2.24×10^{20} 1/Ωms) for spin up (spin down), for $CaFe_4Sb_{12}$ is 2.70×10^{20} 1/Ωms (2.25×10^{20} 1/Ωms) for spin up (spin down), whereas for $SrFe_4Sb_{12}$ is 2.79×10^{20} 1/Ωms (2.17×10^{20} 1/Ωms) for spin up (spin down).

3.4. Electronic thermal conductivity

Both conduction electrons and phonon vibrations are responsible for the thermal conductivity in materials and therefore the total thermal conductivity (κ) can be calculated from the sum of electronic thermal conductivity (κ_e) and thermal conductivity of the phonons (k_l), *i.e.*, $\kappa = \kappa_e + \kappa_l$. The semiconductor's thermal conductivity is dominated by phonons, however, in metals this contribution is mainly due to electrons or free carriers [68–70]. The electronic thermal conductivity per relaxation time (κ/τ) versus chemical potential at the temperature of 300 K is depicted in Fig. 6 for both spin up and down. In the p-type region, the materials shows a direct response to the chemical potential and with the increase in the chemical potential, κ/τ increases very sharply for all materials. Here, increase in κ/τ is more for $CaFe_4Sb_{12}$ with the peak value 11.38×10^{14} W/mKs (12.75×10^{14} W/mKs) for spin up (spin down) followed by $BaFe_4Sb_{12}$ with the peak value of

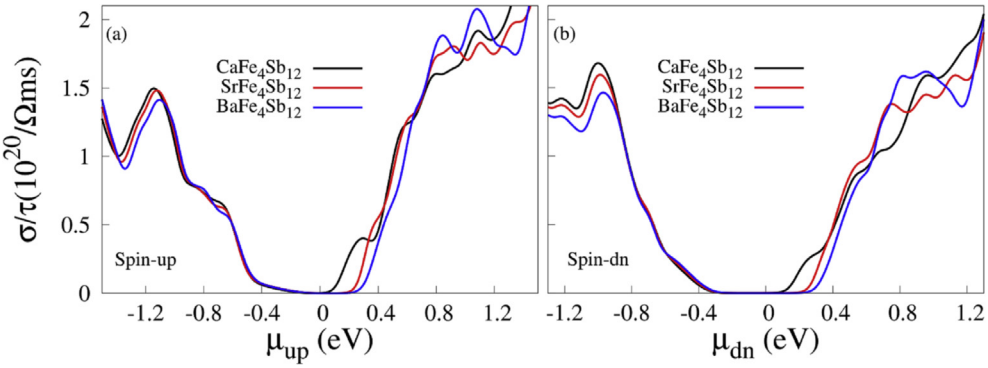

Fig. 5. The ratio of electrical conductivity to relaxation time of $CaFe_4Sb_{12}$, $SrFe_4Sb_{12}$ and $BaFe_4Sb_{12}$versus chemical potential at 300 K for (a) spin up states and (b) spin down states.

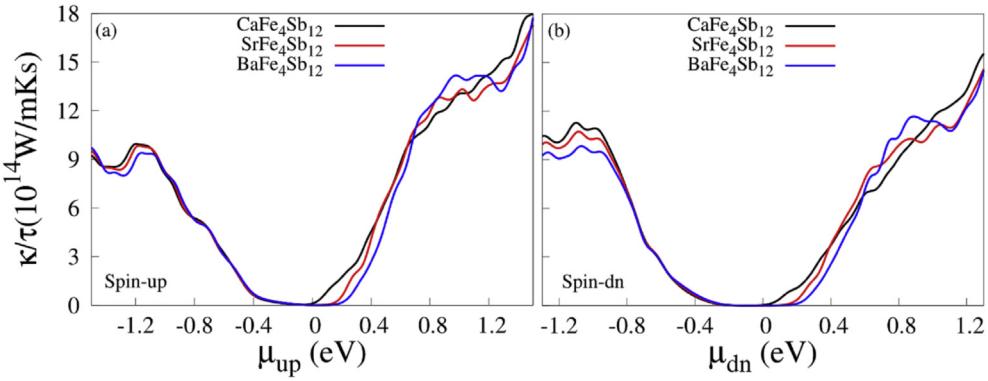

Fig. 6. The ratio of thermal conductivity to relaxation time of $CaFe_4Sb_{12}$, $SrFe_4Sb_{12}$ and $BaFe_4Sb_{12}$versus chemical potential at 300 K for (a) spin up states and (b) spin down states.

10.08×10^{14} W/mKs (10.04×10^{14} W/mKs) for spin up (spin down) and the maximum value obtained of κ/τ value for $SrFe_4Sb_{12}$ is 11.10×10^{14} W/mKs (12.03×10^{14} W/mKs) for spin up (spin down). For the n-type the κ/τ has significant response compared to the p-type region at 300 K temperature. Similar to p-type region as chemical potential is increased in n-type region, an abrupt increase in the κ/τ occurs having the same increase for all materials $CaFe_4Sb_{12}$, $SrFe_4Sb_{12}$ and $BaFe_4Sb_{12}$. Thereafter, for spin up (spin down) calculation the increase is more significant for $BaFe_4Sb_{12}$ ($CaFe_4Sb_{12}$).

The maximum value of 19.88×10^{14} W/mKs (15.78×10^{14} W/mKs) for spin up (spin down) of $BaFe_4Sb_{12}$, followed by maximum peak for $CaFe_4Sb_{12}$with the value of 18.59×10^{14} W/mKs (16.00×10^{14} W/mKs) for spin up (spin down) and for $SrFe_4Sb_{12}$ the maximum value of κ/τ is 19.12×10^{14} W/mKs (15.47×10^{14} W/mKs) for spin up (spin down).

3.5. Power factor

Power factor (PF) compared to Seebeck coefficient and electrical conductivity is the more comprehensive parameter to investigate the thermoelectric performance of a material. Mathematically it is given as $PF = S^2\sigma$, where S is the Seebeck coefficient and σ is the electrical conductivity of a given material. Since in this study we calculate the σ/τ so our reported results for power factor are also PF/τ.

Chemical potential dependence of PF/τ for spin up and down of AFe_4Sb_{12} (A=Ca, Sr and Ba) is shown in Fig. 7. The PF/τ has been

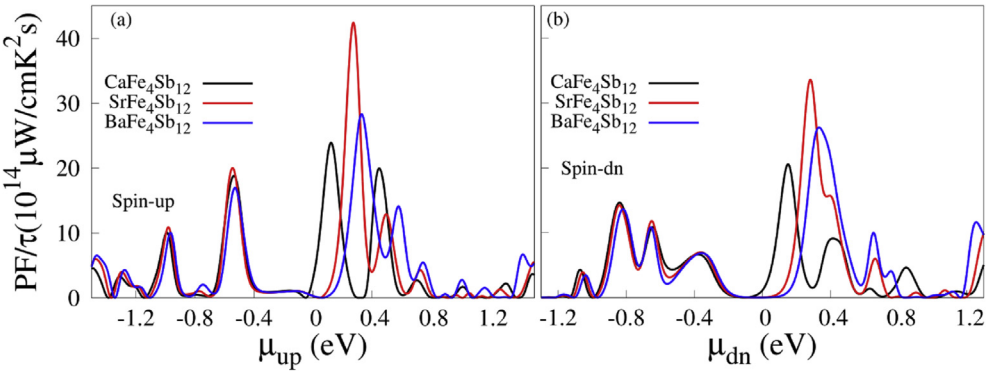

Fig. 7. The ratio of Power Factor (PF) to relaxation time of $CaFe_4Sb_{12}$, $SrFe_4Sb_{12}$ and $BaFe_4Sb_{12}$ versus chemical potential at 300 K for (a) spin up states and (b) spin down states.

taken in units of $10^{14}\mu W/cmK^2s$. The PF/τ is maximum in the chemical potential interval of [−0.1, 0.1 eV]. Therefore, the latter interval can be considered as a critical region for the high performance of alkaline-earth based thermoelectric materials AFe_4Sb_{12} (A=Ca, Sr and Ba). For the p-type region, the PF/τ is negligible for the chemical potential close to −1.0 eV in all the materials under study. This PF/τ's value continuous to remain small up to when chemical potential reaches to the value −0.96 eV. Afterwards the PF starts to fluctuate. In the p-type region, $SrFe_4Sb_{12}$ has higher PF/τ value than those of $CaFe_4Sb_{12}$ and $BaFe_4Sb_{12}$ for spin up, which indicates that the holes contribution with spin up in the p-type region is more for $SrFe_4Sb_{12}$, while for the spin down, $CaFe_4Sb_{12}$ PF is slightly higher than that of the others. In the p-type region, the highest PF value for spin up (spin down) of $SrFe_4Sb_{12}$ is $20.02 \times 10^{14}\mu W/cmK^2s$ ($14.23 \times 10^{14}\mu W/cmK^2s$) at $\mu_{up} = -0.545$ ($\mu_{dn} = -0.840$) eV, and then PF/τ reaches to its maximum value of $18.81 \times 10^{14}\mu W/cmK^2s$ ($14.64 \times 10^{14}\mu W/cmK^2s$) for spin up (spin down) of $CaFe_4Sb_{12}$ at $\mu_{up} = -0.536$ ($\mu_{dn} = -0.839$) eV and finally the maximum of PF/τ of $BaFe_4Sb_{12}$ is $16.96 \times 10^{14}\mu W/cmK^2s$ ($13.63 \times 10^{14}\mu W/cmK^2s$) for spin up (spin down) at $\mu_{up} = -0.527$ ($\mu_{dn} = -0.819$) eV. Similarly, for the n-type region, the same characteristics of the PF/τ values are obtained and compounds favor low doping, however, high PF values are obtained in n-type region than p-type which indicates the prominence of n-type on p-type doping and also of spin up on spin down states in these materials. The maximal value of the calculated PF_{max}/τ in the n-type region for $CaFe_4Sb_{12}$ is $23.91 \times 10^{14}\mu W/cmK^2s$ ($20.54 \times 10^{14}\mu W/cmK^2s$) for spin up (spin down) at $\mu_{up} = 0.122$ ($\mu_{dn} = 0.150$) eV. The PF_{max}/τ is $42.43 \times 10^{14}\mu W/cmK^2s$ ($33.57 \times 10^{14}\mu W/cmK^2s$) at $\mu_{up} = 0.274$ (0.281) eV for spin up (spin down) of $SrFe_4Sb_{12}$. The latter PF_{max} is the highest value which is obtained among these alkaline-earth based skutterudite systems AFe_4Sb_{12} for both spin up and down states. And finally the PF_{max}/τ in n-type region for $BaFe_4Sb_{12}$is $28.30 \times 10^{14}\mu W/cmK^2s$ ($26.22 \times 10^{14}\mu W/cmK^2s$) for spin up (spin down) at $\mu_{up} = 0.329$ ($\mu_{dn} = 0.332$ eV. The value of PF/τ in n-type region shows a decline as the chemical potential increases and becomes negligible at 1 eV chemical potential. It is seen that the calculated PF/τ rapidly increases with increase of doping in the low values of doping region; moreover the n-type doping increases faster than p-doping. Therefore, to improve the Power factor in AFe_4Sb_{12}, the low doping should be used.

4. Conclusions

Thermoelectric study of alkaline-earth elements Ca, Sr and Ba filled antimonide based skutterudite structured compounds is carried out to understand the thermoelectric performance at different chemical potentials for p- and n-type doping at the spin up and down states. It is found that n-type doping is more favorable than p-type doping for these compounds for both spin channels. Furthermore, among the n-type doped materials spin down of $SrFe_4Sb_{12}$ with $PF_{max}/\tau = 42.43 \times 10^{14}\ \mu W/cmK^2s$ is found to be more attractive for the possible thermoelectric applications compared to $CaFe_4Sb_{12}$ and $BaFe_4Sb_{12}$. The result obtained estimates that chemical potential well affects the thermoelectric parameters of these compounds. The effective range for the best thermoelectric application is small doping level for n-type $SrFe_4Sb_{12}$ at the chemical potential $\mu_{up} = 0.274$ (0.281) eV for the spin (down) states respectively.

Acknowledgement

We acknowledge the financial support from the Higher Education Commission, Pakistan (HEC), project No. 20-3959/NRPU/R&D/HEC2014/119.

References

[1] X. Shi, J. Yang, J.R. Salvador, M. Chi, J.Y. Cho, H. Wang, S. Bai, J. Yang, W. Zhang, L. Chen, J. Am. Chem. Soc. 133 (2011) 7837–7846.
[2] A.H. Reshak, RSC Adv. 5 (2015) 33632–33638.
[3] A.H. Reshak, J. Appl. Phys. 117 (2015) 225104–225110.
[4] A.H. Reshak, RSC Adv. 6 (2016) 72286–72294.
[5] M.-S. Lee, S.D. Mahanti, Phys. Rev. B 85 (2012) 165149–615156.
[6] A.H. Reshak, J. Alloy Compd. 670 (2016) 1–11.
[7] A.H. Reshak, RSC Adv. 6 (2016) 54001–54012.
[8] G.J. Snyder, E.S. Toberer, Nat. Mater. 7 (2008) 105–114.
[9] R. Venkatasubramanian, E. Siivola, T. Colpitts, B. O'Quinn, Nature 413 (2001) 597–602.
[10] T.C. Harman, P.J. Taylor, M.P. Walsh, B.E. LaForge, Science 297 (2002) 2229–2232.
[11] B. Poudel, Q. Hao, Y. Ma, Y.C. Lan, A. Minnich, B. Yu, X. Yan, D.Z. Wang, A. Muto, D. Vashaee, X.Y. Chen, J.M. Liu, M.S. Dresselhaus, G. Chen, Z. Ren, Science 320 (2008) 634–638.
[12] M. Zhou, J.F. Li, T.J. Kita, J. Am. Chem. Soc. 130 (2008) 4527–4532.
[13] K.F. Hsu, S. Loo, F. Guo, W. Chen, J.S. Dyck, C. Uher, T. Hogan, E.K. Polychroniadis, M.G. Kanatzidis, Science 303 (2004) 818–821.
[14] B.C. Sales, D. Mandrus, R.K. Williams, Science 272 (1996) 1325–1328.
[15] X. Shi, H. Kong, C.P. Li, C. Uher, J. Yang, J.R. Salvador, H. Wang, L. Chen, W. Zhang, Appl. Phys. Lett. 92 (2008) 182101–182103.
[16] J.P. Heremans, V. Jovovic, E.S. Toberer, A. Saramat, K. Kurosaki, A. Charoenphakdee, S. Yamanaka, G.J. Snyder, Science 321 (2008) 554–557.
[17] B. Poudel, Q. Hao, Y. Ma, Y. Lan, A. Minnich, B. Yu, X. Yan, D. Wang, A. Muto, D. Vashaee, X. Chen, J. Liu, M.S. Dresselhaus, G. Chen, Z. Ren, Science 320 (2008) 634–638.
[18] K. Biswas, J. He, I.D. Blum, C. Wu, T.P. Hogan, D.N. Seidman, V.P. Dravid, M.G. Kanatzidis, Nature 489 (2012) 414–418.
[19] D. Parker, X. Chen, D.J. Singh, Phys. Rev. Lett. 110 (2013) 146601–146605.
[20] W. Zhao, P. Wei, Q. Zhang, H. Peng, W. Zhu, D. Tang, J. Yu, H. Zhou, Z. Liu, X. Mu, D. He, J. Li, C. Wang, X. Tang, J. Yang, Nat. Commun. 6 (2015) 6197–7003.
[21] B.C. Sales, D.G. Mandrus, B.C. Chakoumakos, in: T.M. Tritt (Ed.), Recent Trends in Thermoelectric Materials Research II, Semiconductors and Semimetals, vol. 69, Academic Press, San Diego, 2000, pp. 1–36.
[22] D.T. Morelli, G.P. Meisner, J. Appl. Phys. 77 (1995) 3777–3781.
[23] C. Uher, in: T.M. Tritt (Ed.), Recent Trends in Thermoelectric Materials Research II, Semiconductors and Semimetals, vol. 69, Academic Press, San Diego, 2000, pp. 139–253.
[24] X. Shi, W. Zhang, L.D. Chen, J. Yang, Phys. Rev. Lett. 95 (2005) 185503.
[25] J.L. Feldman, P. Dai, T. Enck, B.C. Sales, D. Mandrus, D. Singh, Phys. Rev. B 73 (2006) 014306.
[26] J.L. Feldman, D.J. Singh, Phys. Rev. B 53 (1996) 6273.
[27] J.L. Feldman, D.J. Singh, Phys. Rev. B 54 (1996) 712E.
[28] R.P. Hermann, R. Jin, W. Schweika, F. Grandjean, D. Mandrus, B.C. Sales, G.J. Long, Phys. Rev. B 90 (2003) 135505.
[29] C.A. Kendziora, G.S. Nolas, Mater. Res. Soc. Symp. Proc. 793 (2004) 107.
[30] L. Nordstrom, D.J. Singh, Phys. Rev. B 53 (1996) 1103–1108.
[31] J.-P. Fleurial, A. Borshchevsky, T. Caillat, in: Proceedings of the 15th International Conference of Thermoelectrics, IEEE, New York, 1996, p. 91.
[32] J.-P. Fleurial, T. Caillat, A. Borshchevsky, in: Proceedings of the 16th International Conference of Thermoelectrics, IEEE, New York, 1997, p. 1.
[33] M.D. Hornbostel, E.J. Hyer, J. Thiel, D.C. Johnson, J. Am. Chem. Soc. 119 (1997) 2665–2668.
[34] D.M. Rowe, V.L. Kuznetsov, L.A. Kuznetsova, in: Proceedings of the, 17th International Conference of Thermoelectrics, IEEE, New York, 1998, p. 323.
[35] X.F. Tang, L.D. Chen, T. Goto, T. Hirai, J. Mater. Res. 16 (2001) 837–843.
[36] X.F. Tang, L.D. Chen, T. Goto, T. Hirai, R.Z. Yuan, J. Mater. Sci. 36 (2001) 5435–5439.
[37] A.H. Reshak, J. Alloys. Compd. 651 (2015) 176–183.
[38] G.S. Nolas, M. Kaeser, R.T. Littleton, T.M. Tritt, Appl. Phys. Lett. 77 (2000) 1855–1857.
[39] L.D. Chen, T. Kawahara, X.F. Tang, T. Goto, T. Hirai, J.S. Dyck, W. Chen, C. Uher, J. Appl. Phys. 90 (2001) 1864–1868.
[40] V.L. Kuznetsov, L.A. Kuznetsova, D.M. Rowe, J. Phys. Condens. Matter 15 (2003) 5035.
[41] Y.Z. Pei, L.D. Chen, W. Zhang, X. Shi, S.Q. Bai, X.Y. Zhao, Z.G. Mei, X.Y. Li, Appl. Phys. Lett. 89 (2006) 221107–221109.
[42] J. Yang, W. Zhang, S.Q. Bai, Z. Mei, L.D. Chen, Appl. Phys. Lett. 90 (2007) 192111–192113.
[43] S.Q. Bai, Y.Z. Pei, L.D. Chen, W.Q. Zhang, X.Y. Zhao, J. Yang, Acta Mater 57 (2009) 3135–3139.
[44] D. Bérardan, E. Alleno, C. Godart, M. Puyet, B. Lenoir, R. Lackner, E. Bauer, L. Girard, D. Ravot, J. Appl. Phys. 98 (2005) 033710–033715.
[45] X. Tang, H. Li, Q.J. Zhang, M. Niino, T. Goto, J. Appl. Phys. 100 (2006) 123702–123709.
[46] P.N. Alboni, X. Ji, J. He, N. Gothard, T.M. Tritt, J. Appl. Phys. 103 (2008) 113707–113711.
[47] D.J. Braun, W. Jeitschko, J. Less Common Met. 72 (1980) 147–156.
[48] C.B.H. Evers, W. Jeitschko, L. Boonk, D.J. Braun, T. Ebel, U.D. Scholz, J. Alloys. Comp. 224 (1995).

[49] V. Keppens, D. Mandrus, B.C. Sales, B.C. Chakoumakos, P. Dai, R. Coldea, M.B. Maple, D.A. Gajewski, E.J. Freeman, S. Bennington, Nature 395 (1998) 876–878.
[50] N.R. Dilley, E.J. Freeman, E.D. Bauer, M.B. Maple, Phys. Rev. B 58 (1998) 6287–6290.
[51] J.W. Kaiser, W. Jeitschko, J. Alloys. Comp. 291 (1999) 66–72.
[52] N.R. Dilley, E.D. Bauer, M.B. Maple, S. Dordevic, D.N. Basov, F. Freibert, T.W. Darling, A. Migliori, B.C. Chakoumakos, B.C. Sales, Phys. Rev. B 61 (2000) 4608–4614.
[53] E. Bauer, St Berger, Ch Paul, M. Della Mea, G. Hilscher, H. Michor, M. Reissner, W. Steiner, A. Grytsiv, P. Rogl, E.W. Scheidt, Phys. Rev. B 66 (2002) 214421–214429.
[54] A. Leithe-Jasper, W. Schnelle, H. Rosner, M. Baenitz, A. Rabis, A.A. Gippius, E.N. Morozova, H. Borrmann, U. Burkhardt, R. Ramlau, U. Schwarz, J.A. Mydosh, Y. Grin, Phys. Rev. B 70 (2004) 214418–214429.
[55] J. Sichelschmidt, V. Voevodin, H.J. Im, S. Kimura, H. Rosner, A. Leithejasper, W. Schnelle, U. Burkhardt, J.A. Mydosh, Yu Grin, F. Steglich, Phys. Rev. Lett. 96 (2006) 037406–037409.
[56] W. Schnelle, A. Leithe-Jasper, H. Rosner, R. Cardoso-Gil, R. Gumeniuk, D. Trots, J.A. Mydosh, Yu Grin, Phys. Rev. B 77 (2008) 094421–094436.
[57] M.M. Koza, M.R. Johnson, R. Viennois, H. Mutka, L. Girard, D. Ravot, Nat. Mater 7 (2008) 805–810.
[58] M. Ueda, Y. Kawahito, K. Tanaka, D. Kikuchi, H. Aoki, H. Sugawara, K. Kuwahara, Y. Aoki, H. Sato, Phys. B 403 (2008) 881–883.
[59] J.P. Perdew, A. Ruzsinszky, G. Csonka, O.A. Vydrov, G.E. Scuseria, L.A. Constantin, X. Zhou, K. Burke, Phys. Rev. Lett. 100 (2008) 136406–136411.
[60] P. Blaha, K. Schwarz, G. Madsen, D. Kvasnicka, J. Luitz, WIEN2k, an Augmented Plane Wave Plus Local Orbitals Program for Calculating Crystal Properties User's Guide, WIEN2k 14.2, 2014. Vienna University of Technology, Inst. of Physical and Theoretical Chemistry Getreidemarkt 9/156, A-1060 Vienna/Austria.
[61] P.B. Allen, Boltzmann theory and resistivity of metals, in: J.R. Chelikowsky, S.G. Louie (Eds.), Quantum Theory of Real Materials, Kluwer, Boston, 1996, pp. 219–250.
[62] G.K.H. Madsen, D.J. Singh, Comp. Phys. Commun. 175 (2006) 67–71.
[63] B. Khan, H.A.R. Aliabad, N. Razghandi, M. Maqbool, S.J. Asadabadi, I. Ahmad, Comp. Phys. Commun. 187 (2015) 1–7.
[64] P.F. Qiu, J. Yang, R.H. Liu, X. Shi, X.Y. Huang, G.J. Snyder, W. Zhang, L.D. Chen, J. Appl. Phys. 109 (2011) S063713–S063720.
[65] Z.-z. Cheng, Z. Cheng, M.-h. Wu, J. Magn. Magn. Mater 320 (2008) 2591–2595.
[66] A. Zhou, L.-S. Liu, C.-C. Shu, P.-C. Zhai, W.-Y. Zhao, Q.-J. Zhang, J. Elect. Mater 40 (2011) 974–979.
[67] W. Schnelle, A. Leithe-Jasper, H. Rosner, R. Cardoso-Gil, R. Gumeniuk, D. Trots, J.A. Mydosh, Yu Grin, Phys. Rev. B 77 (2008), 094421–16.
[68] C. Kittel, Introduction to Solid State Physics, eighth ed., John Wiley & Sons, Hoboken, USA, 2004, p. 156.
[69] M. Bilal, I. Ahmad, S.J. Asadabadi, R. Ahmad, M. Maqbool, Electron. Mater. Lett. 11 (3) (2015) 466–480.
[70] T.M. Tritt, Thermal Conductivity: Theory, Properties, and Applications, Kluwer Academic/PLENUMpublishers, New York, USA, 2004, p. 75.